



HAL
open science

A dynamic and collaborative database for morphogeometric information of trilobites

Fernanda Serra, Diego Balseiro, Claude Monnet, Enrique Randolfe, Arnaud Bignon, Juan J Rustán, Valentin Bault, Diego F Muñoz, N. Emilio Vaccari, Malena Martinetto, et al.

► To cite this version:

Fernanda Serra, Diego Balseiro, Claude Monnet, Enrique Randolfe, Arnaud Bignon, et al.. A dynamic and collaborative database for morphogeometric information of trilobites. *Scientific Data* , 2023, 10 (1), pp.841. 10.1038/s41597-023-02724-9 . hal-04418979

HAL Id: hal-04418979

<https://hal.science/hal-04418979>

Submitted on 26 Jan 2024

HAL is a multi-disciplinary open access archive for the deposit and dissemination of scientific research documents, whether they are published or not. The documents may come from teaching and research institutions in France or abroad, or from public or private research centers.

L'archive ouverte pluridisciplinaire **HAL**, est destinée au dépôt et à la diffusion de documents scientifiques de niveau recherche, publiés ou non, émanant des établissements d'enseignement et de recherche français ou étrangers, des laboratoires publics ou privés.



Distributed under a Creative Commons Attribution 4.0 International License



OPEN

DATA DESCRIPTOR

A dynamic and collaborative database for morphogeometric information of trilobites

Fernanda Serra ^{1,2}, Diego Balseiro ^{1,2}, Claude Monnet ³, Enrique Randolfe ^{1,2}, Arnaud Bignon ^{1,2}, Juan J. Rustán ^{1,2}, Valentin Bault ³, Diego F. Muñoz ^{4,5}, N. Emilio Vaccari ^{1,2}, Malena Martinetto¹, Catherine Crônier ³✉ & Beatriz G. Waisfeld ^{1,2}✉

Modern morphometric-based approaches provide valuable metrics to quantify and understand macroevolutionary and macroecological patterns and processes. Here we describe TriloMorph, an openly accessible database for morpho-geometric information of trilobites, together with a landmark acquisition protocol. In addition to morphological traits, the database contains contextual data on chronostratigraphic age, geographic location, taxonomic information and lithology of landmarked specimens. In this first version, the dataset has broad taxonomic and temporal coverage and comprises more than 55% of all trilobite genera and 85% of families recorded in the Paleobiology Database through the Devonian. We provide a release of geometric morphometric data of 277 specimens linked to published references. Additionally, we established a Github repository for constant input of morphometric data by multiple contributors and present R functions that help with data retrieval and analysis. This is the first attempt of an online, dynamic and collaborative morphometric repository. By bringing this information into a single open database we enhance the possibility of performing global palaeobiological research, providing a major complement to current occurrence-based databases.

Background & Summary

Understanding biotic responses to large scale environmental changes -either past or recent- is one of the main goals of macroecology and macroevolution. Major biological events that took place during the Palaeozoic, such as the Cambrian Explosion, the Great Ordovician Biodiversification Event (GOBE), and the mid-Palaeozoic Marine Revolution, shaped the marine life for the rest of the Phanerozoic and paved the way for the forthcoming configuration of current marine ecosystems¹⁻⁴. Among the iconic organisms of this Era, trilobites are a fundamental group for the study of Palaeozoic benthic faunas and provide excellent opportunities for the understanding of mechanisms underlying ecological and evolutionary patterns at different spatial and temporal scales⁵⁻⁹. Several palaeontological studies have highlighted the critical role of trilobites in the signature of the Cambrian-Ordovician ecosystems and, although declined significantly during the Late Ordovician extinction, they continued being an emblematic group of the benthic ecosystems during the middle Palaeozoic¹⁰.

Palaeobiodiversity studies have classically examined taxonomic changes on the basis of the fossil record¹¹⁻¹⁵. Indeed, understanding the patterns of diversity collapses and recoveries provides valuable insights into drivers of changes and helps to inform conservation activities in modern marine ecosystems in light of anthropogenic climate change^{16,17}. Most of these studies are facilitated by the Paleobiology Database¹⁸ (PBDB) or the Geobiodiversity Database¹⁹ (GBDB), which are comprehensive, international collaborative, taxonomic and occurrence databases already available and widely used to assess macroevolutionary patterns and processes in deep time and for global to regional analyses²⁰⁻²⁴. Related studies, therefore, focused mainly on the taxonomic richness component of biodiversity. However, it is well-known that

¹Universidad Nacional de Córdoba, Facultad de Ciencias Exactas Físicas y Naturales, Córdoba, Argentina. ²CICTERRA (Centro de Investigaciones en Ciencias de la Tierra), CONICET, Córdoba, Argentina. ³Univ. Lille, CNRS, UMR 8198 – Evo-Eco-Paleo, F-59000, Lille, France. ⁴IIMYC (Instituto de Investigaciones Marinas y Costeras), CONICET - Universidad Nacional de Mar del Plata, Mar del Plata, Argentina. ⁵IGCyC (Instituto de Geología de Costas y del Cuaternario), Universidad Nacional de Mar del Plata - CIC PBA, Mar del Plata, Argentina. ✉e-mail: catherine.cronier@univ-lille.fr; bwaisfeld@unc.edu.ar

biological diversity is multifaceted (e.g.²⁵), and morphological diversity is another key aspect to understanding ecological-evolutionary patterns in deep time²⁶.

For extinct organisms such as trilobites, morphological disparity is highly relevant to understand and quantify macroevolutionary and macroecological patterns and processes (e.g.^{5,27–30}). Modern morphometric-based approaches, such as landmarks and morphospaces, are also used as valuable metrics to quantify impacts and responses of marine ecosystems to large-scale changes (such as global warming) in terms of morphology and functional needs through deep time (e.g.^{31–37}). Regarding morphological information, only small datasets linked to specific publications exist, while very few large scale morphological datasets are currently available (e.g.^{38–40}). Regarding trilobites, there has been an increase in taxonomically comprehensive morphological databases⁴¹, such as outline data describing the shape of the cranium³¹, semilandmarks describing the shape of the cephalon⁴², landmark and semilandmarks configuration on cephalic outline, glabella and eye ridges⁴³, landmarks and semilandmark data on cephalon and pygidia⁴⁴, as well as trilobite moulting morphometric measurements⁴⁵. Here, we develop a database for morphological information of trilobites that is also quantified by means of geometric morphometrics state-of-the-art methods. These approaches allow objective quantification of shape of organisms, ordinate major shape differences onto morphological spaces, and then quantify the occupation of this morphospace by various disparity metrics and compare them to phylogenetic patterns or known abiotic and biotic changes. The novelty behind TriloMorph is its dynamic and collaborative nature, thus promoting inclusive and sustainable work between researchers, approaching an open science framework.

Trilobites are extinct marine mostly benthic, mobile organisms forming the class Trilobita, one of the earliest known groups of arthropods. They first appear in the fossil record around 521 Ma ago and flourished throughout the lower Palaeozoic^{46,47}, before slipping into a long decline, with all trilobite orders except the Proetida dying out during the Late Devonian⁴⁸. The last trilobites finally disappeared at the end-Permian mass extinction about 252 Ma ago⁴⁹. Trilobites were among the most successful of all early animals, thriving in oceans for almost 270 million years, with over 20,000 species having been described^{41,50}. Due to their excellent fossil record and high diversity and abundance, they are an ideal group for analysing biotic changes during the Palaeozoic.

In this first release of the openly accessible “TriloMorph” Database, we describe the general landmarking protocol and database functionality (Fig. 1). The initial dataset is focused on Devonian trilobites, and late Cambrian–Early Ordovician ones to a lesser extent, which have a very rich fossil record at times where major transitions of life happened^{10,51}. The morphology of most Devonian trilobite genera with records in the PBDB has been digitized and compiled in the database which, in addition to these morphological traits, contains contextual data on chronostratigraphic age, geographic location, taxonomic information, and lithology of the landmarked specimens. TriloMorph is the first attempt of such an open online morphometric repository of extinct marine organisms that promotes and brings together data generated from the collaborative efforts of contributors in a dynamic manner. The possibility of integrating morphometric data with data from the established Paleobiology Database, which is the biggest online resource of fossil occurrence data, provides the opportunity to address large-scale palaeobiological studies.

Methods

Morphological data were compiled from a landmark-based geometric morphometric approach⁵² to investigate the morphology of two major anatomical structures of trilobites, namely the cephalon and the pygidium. Specimens selected for digitization were compiled from the literature and belong to public collections with a unique repository code. Specimens were named after this alphanumeric identifier and digitised from their original 2D published pictures (Fig. 1, Data recollection). In this sense, 2D landmark configuration has proven to be adequate for capturing shape change in trilobites, despite the differences that may exist in the convexity of certain structures⁵³. Landmarks and semilandmark curves were referred to the right half of the structures analysed, on a dorsal view of each specimen. If a specimen had the left side better preserved, the picture was mirrored prior to landmarking. When missing, a graphic scale was placed on each specimen prior to digitization. Morphology of the cephalon is described by 16 landmarks and 4 semilandmark curves, and the pygidium by 7 landmarks and 3 semilandmark curves (Tables 1, 2, Fig. 2). Geometric morphometrics enables describing the shape of organisms by specifying landmarks, which are homologous topological points identifiable in all studied specimens, as well as semilandmarks, which are equally-spaced points capturing the shape of boundary curves and of surfaces⁵⁴. Semilandmark curves for the cephalon represent the shape of the glabella, cranial and cephalic outlines and the posterior part of the cephalon (Figs. 2, 3). Regarding the pygidium, the semilandmark curves represent the pygidial and axis outlines and the border furrow.

Landmark quantification may vary between specimens depending either on the preservation of the specimen or because the specific trait is not present in the respective taxon; for example eyes in blind taxa or specimens with no articulated cephalon. In the case of an incomplete specimen selected for digitization, for example, a cephalon with a broken genal spine, we completed its morphology by taking in reference another specimen from the same publication. In exceptional cases where certain taxa do not have well preserved structures, drawings were used for digitization if they were based on a specific specimen with a repository code. However, it is frequent that some taxa lack certain structures; in these cases, we suggest removing these traits from the analysis. In the static release, 82% of the specimens in the database allow complete landmark acquisition in the cephalon and 100% in the pygidia. Also, this first release includes only adults (early holaspide and holaspide) specimens.

Landmark and semilandmark selection will ultimately depend on the scope of the analysis. Thereby, here we present a comprehensive digitization protocol.

Several softwares exist for 2D landmark acquisition, such as ‘ImageJ’⁵⁵, ‘tps’ series⁵⁶, or the digitize2d() function in the ‘geomorph’ R package^{57,58}. Here, we used both the ‘digitizeImages()’ function in the ‘StereoMorph’ package⁵⁹ for R⁶⁰, and the classical ‘tpsDig’ software⁵⁶.

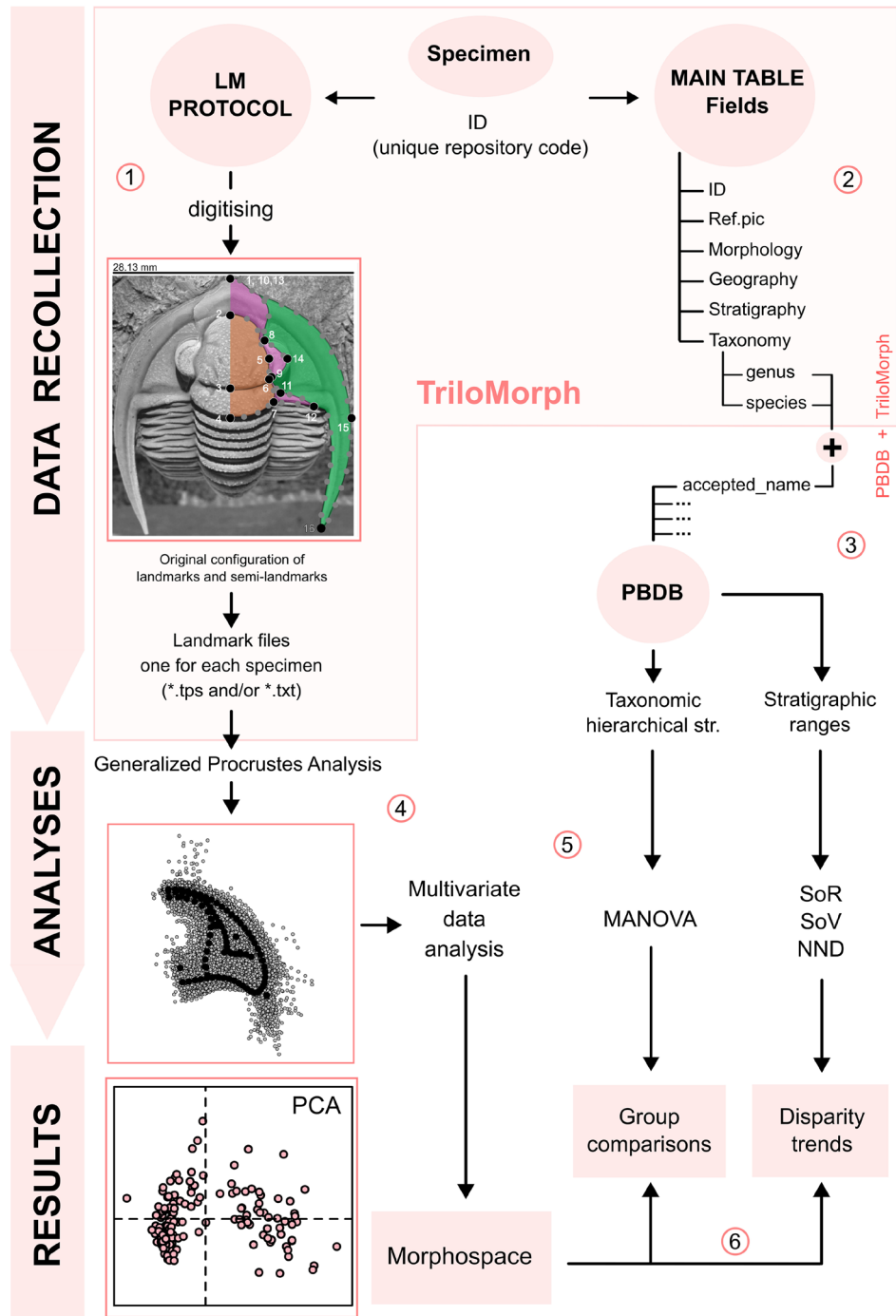


Fig. 1 Flow diagram illustrating the main TriloMorph workflow: (1) LM protocol: the acquisition of morphological data of a specimen with unique repository code (ID) is carried out following the provided landmark protocol; after digitising, one landmark file is generated for each specimen. (2) Main table: specimen ID conforms the basic unit of entry in the main table that contains specimen-level traits and contextual characteristics ('data.csv'). (3) PBDB + TriloMorph: taxonomic hierarchical structure and stratigraphic ranges can be obtained by merging TriloMorph data with occurrence and higher taxonomic information from the PBDB by using the accepted name from PBDB and species or genus names from TriloMorph, (4) Generalised Procrustes analysis: standardisation of landmark data. (5) Analyses: a variety of analytical tools can be used to quantify shape variation (e.g. multivariate data analysis, MANOVA, disparity measures) depending on the research goal. (6) Results: with this database and protocol it is possible to construct a morphospace to visualise patterns of shape variation in trilobites, carry out group comparative analyses or study disparity trends. A step by step explanation of the procedure and R function utilisation is given for the highlighted part (pink box) and an example on the analysis and results sections using Devonian genera from TriloMorph is provided in the R code TriloMorph-workflow. Abbreviations: LM: landmark; Taxonomic Hierarchical str.: Taxonomic Hierarchical structure; SoR: sum of ranges; SoV: sum of variances; NND: Nearest neighbour distance; PCA: principal component analysis.

Landmarks	
Number	Definition
LM1	Antermost point of the sagittal cephalic length without spine
LM2	Antermost point of the sagittal glabellar length
LM3	Intersection between the sagittal axis and the occipital furrow
LM4	Posteriormost point of the sagittal cephalic length
LM5	Maximum transversal glabellar width
LM6	Intersection between the occipital and axial furrows
LM7	Intersection between the posterior margin and the axial furrow
LM8	Antermost end of the eye
LM9	Posteriormost end of the eye
LM10	Anterior facial suture at the sagittal line
LM11	Intersection between the posterior branch of facial suture and the posterior or lateral border furrow
LM12	Intersection between the posterior branch of facial suture and the posterior or lateral margin
LM13	Antermost point of the sagittal (or ex-sagittal) cephalic length (if spiny, LM13 at the tip of the spine)
LM14	Lateralmost external point of the eye
LM15	Cephalic width at the level of the posterior margin of the occipital ring (LM4). If that point cannot be located, it is defined as the extreme of the genal angle (see Fig. 3).
LM16	Tip of the genal angle or spine
Semilandmarks (curves)	
Curve	Starting landmark - ending landmark
Glabella (C.1)	LM2 - LM7
Facial suture (C.2)	LM10 - LM12
Anterior margin (C.3)	LM13 - LM15
Posterior margin (C.4)	LM4 - LM15

Table 1. Definition of the landmarks and semilandmark curves for the cephalon.

Landmarks	
Number	Definition
LM1	Antermost point of the pygidial axis
LM2	Posteriormost point of the pygidial axis
LM3	Border furrow at the sagittal point
LM4	Posteriormost point of pygidium at the sagittal line (if spiny LM 4 at the tip of the spine).
LM5	Intersection between the axial furrow and the anterior pygidial margin
LM6	Intersection between the anterior pygidial margin and the border furrow
LM7	Intersection between the anterior and the lateral pygidial margin
Semilandmarks (curves)	
Curve	Starting landmark - ending landmark
Axis (C.1)	LM1 - LM2
Border furrow (C.2)	LM3 - LM6
Margin (C.3)	LM4 - LM5

Table 2. Definition of the landmarks and semilandmark curves for the pygidium.

Data Records

Here we provide the release of a geometric morphometric dataset of 277 specimens. The associated metadata has information down to specimen level, thus allowing, for example, to include several specimens of the same species for intra-specific analyses. Because it is a specimen-based dataset, TriloMorph allows users to carry out analyses at any desired taxonomic resolution. All specimens included in this release are linked to published references (i.e. peer-reviewed papers, taxonomic monographs, books etc., see references in the GitHub repository) and are derived from localities all around the world (Fig. 4). As a first step, and as a strategy to maximise taxonomic coverage of the dataset, we include one specimen per genus. The current version of the dataset has broad taxonomic and temporal coverage and comprises more than 55% of all trilobite genera and 85% of families in the PBDB in the Devonian geological stages (Fig. 5) and even some taxa yet lacking occurrences in the PBDB. Static releases of the database are available directly from the Universidad Nacional de Córdoba data repository⁶¹ and Zenodo⁶², while a dynamic collaborative version is available in GitHub (<https://github.com/balsedie/trilomorph>). The purpose of the TriloMorph GitHub repository is to allow the constant input of new data into the database. We also provide a step by step explanation of the procedure to upload new data and describe the

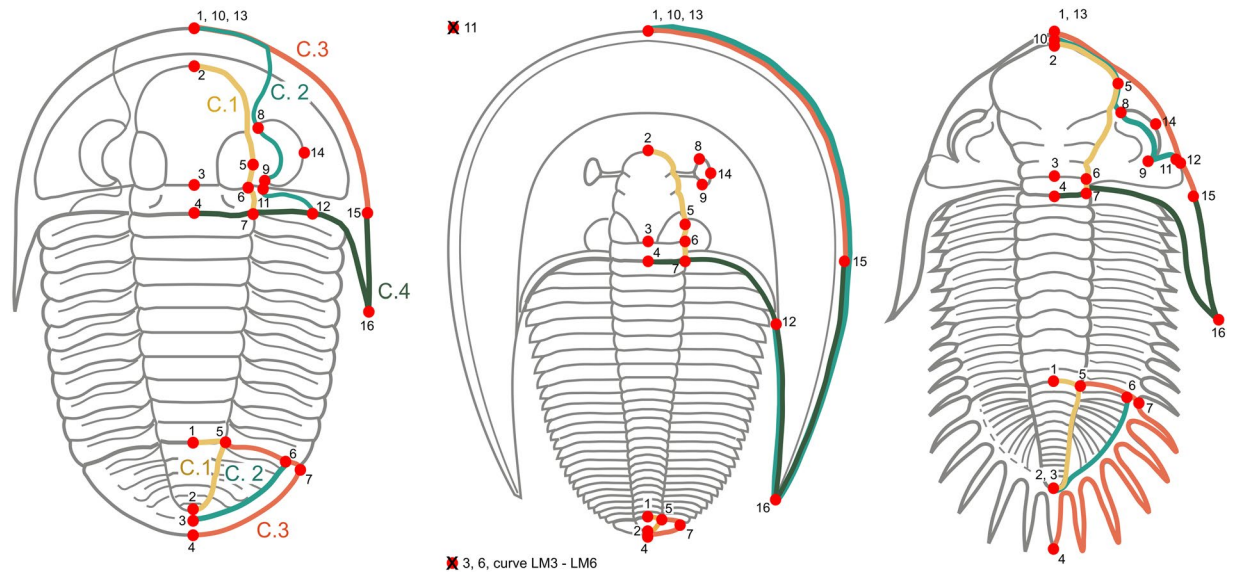


Fig. 2 Template of landmarks and semilandmarks curves used in the TriloMorph database illustrated on three different genera (*Cyphoproetus*, *Harpes*, and *Kayserops*, from the left to the right). For *Harpes*, absent landmarks are referred to as crosses besides the figure. Figures adapted from Gon, S.M. III¹¹⁴, used with permission.

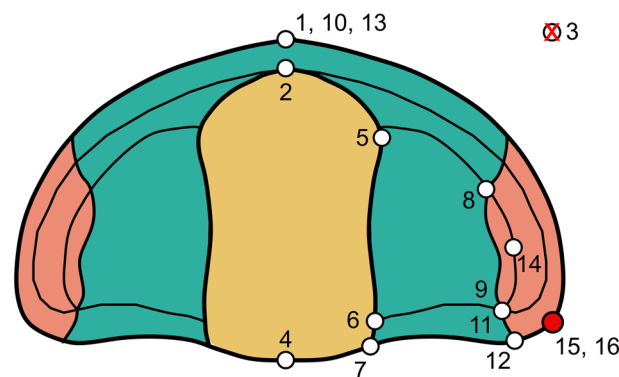


Fig. 3 Schematic diagram of the cephalon of *Ellipsocephalus*, showing the alternative position of LM 15 in the template used in the geometric morphometric analysis. Figure adapted from Gon, S.M. III¹¹⁴, used with permission.

R functions needed to download and analyse data hosted in this repository. Static releases are in the form of a compressed folder containing the following files and folders:

Metadata. YAML file containing the contextual information of considered specimens (see below and Table 3). YAML is a human-friendly data serialisation language for all programming languages⁶³.

References.csv. A CSV-formatted file containing the bibliographic information of data sources. Each entry of the specimen-based table ('data.csv') contains the identification number of the data source, whose bibliographic details are provided in this 'reference.csv' table, which can then be used for citation purposes and should be credited in subsequent publications using the database. Contributors are also acknowledged in the accompanying file 'contributors.csv'.

Images. A folder containing the digitised images. Image files are named after the specimen identification number (i.e., collection/repository number, also present in the main table 'data.csv'), and are appended with a suffix to identify the corresponding anatomic structure of the trilobite ("_C" and "_P" for the cephalon and the pygidium, respectively). File names should not contain spaces. All pictures have a graphical scale. Available formats are JPG and PNG. Images of cephalata and pygidia are saved in different subfolders.

Landmarks. A folder containing the shape data (landmarks and semilandmark curves) for each specimen separately. Similarly to images, landmark files are named after the repository code of the corresponding specimen

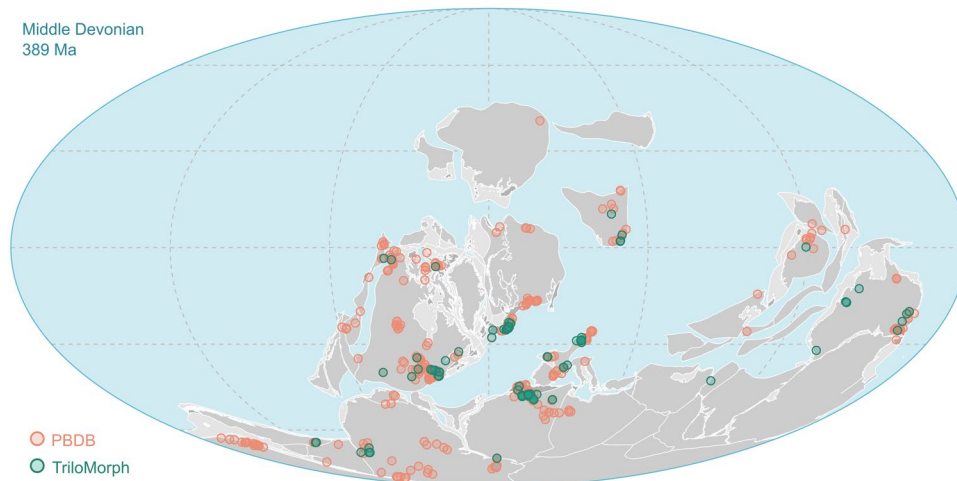


Fig. 4 Palaeogeographic map of the Eifelian Stage (Middle Devonian) indicating the geographic location of the studied collections of trilobite specimens included in the TriloMorph database (green) and location of collections from the PBDB (pink) in order to show the geographic coverage of TriloMorph. Palaeogeography is reconstructed using the PALEOMAP model¹¹⁵ in GPlates¹¹⁶.

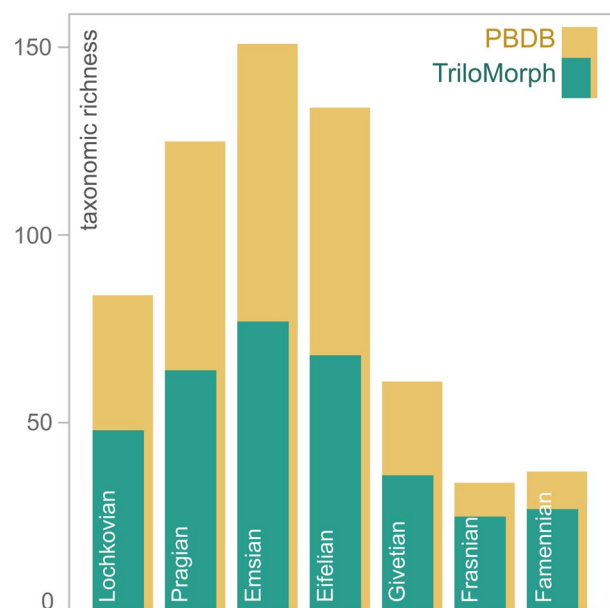


Fig. 5 Amount of genera documented in the TriloMorph database (green) in relation to the number of trilobite genera for each Devonian stage recorded in the PBDB (yellow). Taxonomic richness was range standardised based on the Devonian occurrences recorded in the PBDB.

appended with the suffix of the considered morphological structure (see above). Shape files created with StereoMorph (*.txt) or tpsDig (*.tps) are available. Shape files of cephalon and pygidia are saved in different subfolders.

The database is, therefore, a collection of data files overseen by a main table designed to contain specimen-level traits for considered taxa. The basic unit of entry in this main table is that of a specimen, normally stored in public collections and with a unique alphanumeric identifier (**id**), that is also accompanied by contextual characteristics such as the publication describing this specimen (**ref.pic**), taxonomic information (**taxonomy.genus**, **taxonomy.orig_genus**, **taxonomy.gen_status**, **taxonomy.gen_author**, **taxonomy.subgen**, **taxonomy.sp**, **taxonomy.orig_sp**, **taxonomy.sp_author**, **taxonomy.subsp**), relevant morphological information (**morphology.cephalon**, **morphology.cranidium**, **morphology.pygidium**, **morphology.eyes**, **morphology.ontogeny**), geographic context (**geography.lat**, **geography.long**, **geography.country**, **geography.state**, **geography.county**), and stratigraphic information (**stratigraphy.formation**, **stratigraphy.min_age**, **stratigraphy.max_age**, **stratigraphy.ref_age**, **stratigraphy.basin**, **stratigraphy.environment**). These metadata are crucial for subsequent analyses of morphological disparity in a spatial, temporal and environmental context. Details about each field are described

Field group	Field name	Description
	*ID	Unique specimen collection number (either the official repository number, or, if not available, a combination of the publication information illustrating the specimen (author_year_plate_figure))
	*ref.pic	Reference of the digitised specimen image
	*enter.metadata	person who entered the metadata (format: Surname initials)
	*enter.landmark	person who digitised images (format: Surname initials)
	comments	space to comment on any of the previous fields
Taxonomy	*taxonomy.orig.genus	Original genus assignment in the publication
Taxonomy	*taxonomy.genus	Valid genus name of the specimen
Taxonomy	taxonomy.gen.status	Open nomenclature qualifier for genus identification (such as 'aff', 'cf', or '?', among others)
Taxonomy	taxonomy.gen.author	Author of the genus (surname(s) and year)
Taxonomy	taxonomy.subgen	Valid subgenus name
Taxonomy	taxonomy.orig.sp	Original species assignment in the publication
Taxonomy	*taxonomy.sp	Valid species name (use binomial nomenclature)
Taxonomy	taxonomy.sp.author	Author of the species (surname(s) and year)
Taxonomy	taxonomy.subsp	Valid subspecies name
Morphology	*morphology.cephalon	Boolean value to inform about the digitised structure ('TRUE' if it corresponds to a cephalon, otherwise 'FALSE')
Morphology	*morphology.cranidium	Boolean value to inform about the digitised structure ('TRUE' if it corresponds to a cranidium, otherwise 'FALSE')
Morphology	*morphology.pygidium	Boolean value to inform about the digitised structure ('TRUE' if it corresponds to a pygidium, otherwise 'FALSE')
Morphology	*morphology.eyes	Boolean value to inform if the species has eyes (TRUE) or not (FALSE)
Morphology	*morphology.ontogeny	inform the ontogenetic stage of the specimen (early Holaraspis, Holaraspis, Meraspis)
Geography	*geography.locality	name of the locality from which the specimen was collected
Geography	geography.country	country of origin of the specimen
Geography	*geography.lat	latitude of the locality of origin of the specimen. Format: decimal coordinates
Geography	*geography.long	longitude of the locality of origin of the specimen. Format: decimal coordinates
Geography	geography.state	state of origin of the specimen
Geography	geography.county	county of origin of the specimen
Stratigraphy	stratigraphy.formation	name of the formation from which the specimen comes from
Stratigraphy	*stratigraphy.min_age	minimum age for the occurrence of the specimen (stage)
Stratigraphy	*stratigraphy.max_age	maximum age for the occurrence of the specimen
Stratigraphy	stratigraphy.ref_age	reference for age determination (format: Surname year, Surname Surname year, Surname <i>et al.</i> year)
Stratigraphy	stratigraphy.basin	name of the basin from which the specimen comes from Stratigraphy

Table 3. Definition of the fields describing the specimen-based table of contextual information ('data.csv') (*mandatory fields for subsequent classical analyses).

in Table 3. Although it is not the current scope of the database, the specimen-based structure of the database allows including several specimens of the same species to also perform intraspecific analyses.

In addition to the database, we also provide several R functions to read both StereoMorph and TPS data simultaneously (function 'shapRead' in the file 'trilomorph-funs.R') into a list structure, then to check homogeneity (number of landmarks, number of curves and constituting semilandmarks, presence of a scale, presence of missing landmarks) of the loaded landmark data, next to resample each curve to the same number of semilandmarks as requested by the user (function 'shapFix' in the file 'trilomorph-funs.R') and to finally provide a standard 3D landmark array (landmark values by landmark dimension and by specimen, see⁶⁴). In case of inconsistencies among the selected specimens, the latter function automatically removes these specimens with missing landmarks.

Technical Validation

The acquisition of landmarks for this database used softwares, such as tps⁵⁶ and StereoMorph⁵⁹, which have been abundantly used in palaeontology and biology for decades and have proven to be efficient and accurate, therefore, ensuring technical rigour (e.g.^{52,64}).

The landmark template defined here is the result of a collaborative work among many trilobite specialists in our group (e.g.^{44,48,51,65–86}) and is also based on a long historical research of landmark-based protocols in trilobites (e.g.^{42,84,87–95}). It is designed to maximise trilobite shape description across all major trilobite orders.

One important concern might be the capability of the proposed landmarking protocol to recognize trilobite morphological variation across its whole -or at least most of the- phylogeny but also recognize variability within taxonomic groups. In this sense, our results of the trilobite morphospace indicates that the current protocol is particularly sensitive to the main morphological changes that have been previously described in the literature^{96,97} (Fig. 6). For example, our method is able to capture the cephalon outline, but also suture and glabella outline and eye

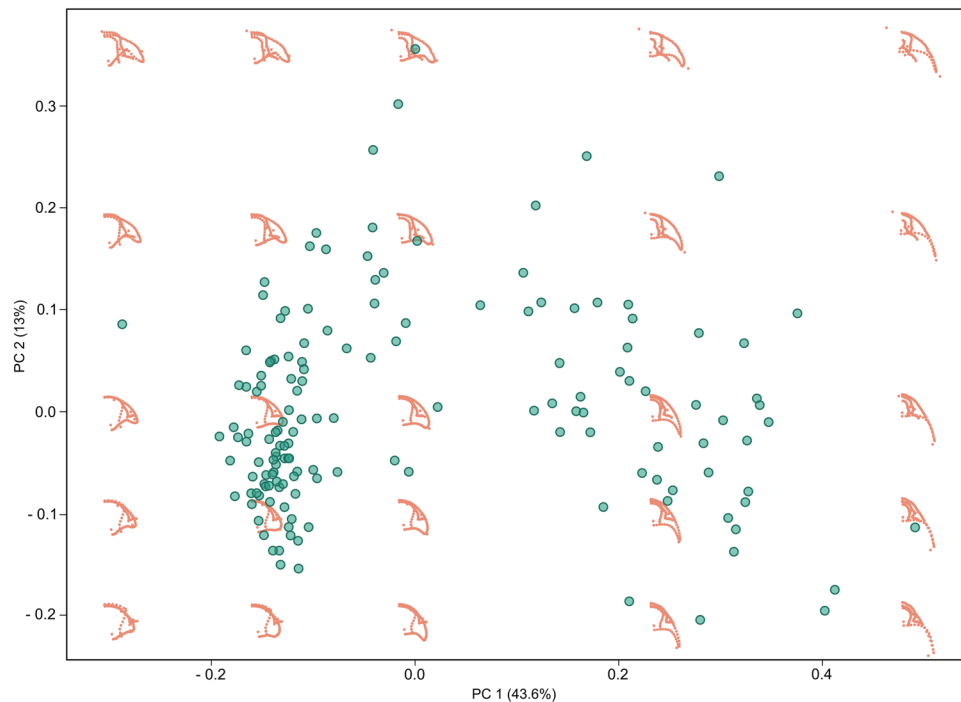


Fig. 6 Trilobite morphospace using Devonian data from TriloMorph, virtual shapes are plotted in order to show intuitively how shape varies across morphospace. Note that our landmarking protocol is particularly sensitive to the main morphological changes described in the literature⁹⁶. For example, the lower right quadrant represents mostly morphological diversity among Phacopidae, towards the upper part mostly Homalonotidae, Styginidae, Calmonidae, towards the lower left quadrant morphological diversity resembles Acastidae, Odontopleuridae, Aulacopleuridae, Proetidae.

morphology, as well as key pygidial features, all of which have been interpreted as important traits when describing the morphological variability among trilobites⁹⁷. Results using this protocol demonstrated its ability to distinguish main morphological variations across all orders and families present during the Devonian (see Usage notes), as well as at regional and local scales during the lower Ordovician⁷⁷, and within a single family (Phacopidae) along its whole evolutionary history⁴⁴.

However, there are some taxonomic groups that represent a challenge for the application of this protocol. For example, in several trilobite clades (e.g. some representatives of the Suborder Illaenina, and the Order Asaphida) effacement of cephalic and pygidial furrows is a common feature, making it difficult to determine certain landmarks and curves. On the other hand, there are several types of facial sutures, and therefore the curves and landmarks involved have been resolved to encompass these different patterns. For instance, for marginal sutures that run along the cephalic margins, LM 10 (anterior facial suture at the sagittal line) is placed together with LM 1 and so the cranial outline is adjacent to the cephalic margin (e.g. harpetids); for sutures running parallel to the anterior border, LM 10 is positioned between LM1 and LM2 so the anterior part of the cranial outline runs parallel to the margin (e.g. dalmanitids) (Fig. 2).

Because the database is based on landmarked data obtained by different contributors and digitising software, we tested for variation on landmarked data as a measurement of data quality. We tested three different sources of error for morphogeometric data, namely within and between observer variability in the landmarking process, and variability between different landmark acquisition software. For this, we compared inter-generic variability in our dataset with variability in a single specimen based on (1) ten landmark and semilandmark configurations obtained by the same observer (within observer variability, two test cases) and (2) landmark and semilandmark configurations obtained by 8 different observers using StereoMorph and one observer using TPS (among observer variability). Morphological variability was estimated as (1) the pairwise Procrustes distances among specimens within each group: among-genus, among-observers and within-observers and (2) total multivariate dispersion in the morphospace for each group. Results indicate that within observer variability, i.e. strict measurement error (0.014 and 0.02), and among observer variability (0.028), which in turn includes different landmark acquisition software variability, are substantially smaller (one order of magnitude) than inter-generic variation (0.35), see Fig. 7.

A Kruskal-Wallis rank test confirms that the differences in pairwise Procrustes distances are statistically significant ($\chi^2 = 349.85$, $df = 3$, $p < 2.2e-16$). The test for multivariate dispersion⁹⁸ also indicates statistically significant differences ($df = 3$, $F = 80.524$, $p < 2.2e-16$). We further used a Tukey test to recognise which groups were significantly different based on their multivariate dispersions. Table 4 indicates that significant differences are present only when comparing inter-generic variability to among-observers and within-observer variabilities

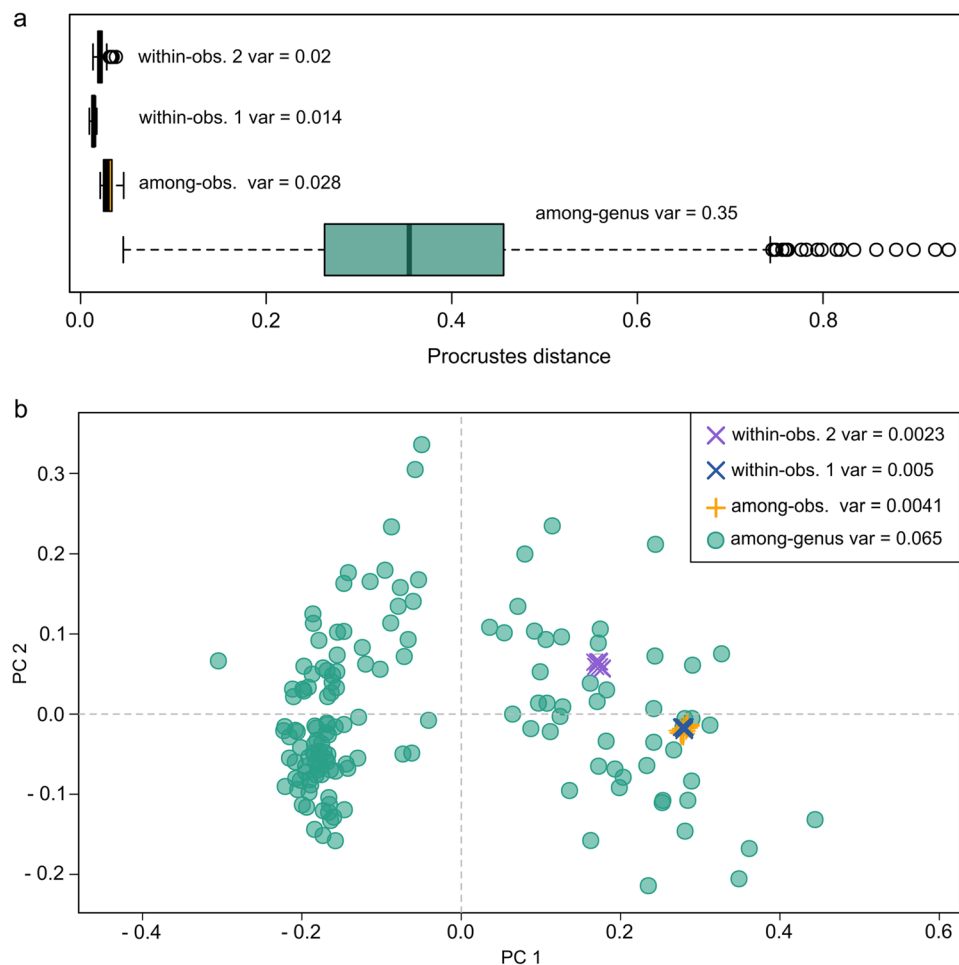


Fig. 7 Morphological variability among specimens from two sources of error for morphogeometric data: within-observer (within-obs. 1, within-obs. 2), and among-observers (among-obs.), compared to among-genus variability. **(a)** Distribution of pairwise Procrustes distances among specimens within each group. **(b)** Morphospace for measurement error for specimens within each group.

Groups	difference	lower	upper	p
among-obs. - among-genus	-0.230	-0.298	-0.162	0*
within-ob.1 - among-genus	-0.236	-0.297	-0.175	0*
within-ob.2 - among-genus	-0.232	-0.294	-0.171	0*
within-ob.1 - among-obs	-0.006	-0.095	0.083	0.998
within-ob.2 - among-obs	-0.002	-0.092	0.087	0.999
within-ob.2 - within-ob.1	0.004	-0.080	0.088	0.999

Table 4. Tukey test performed to identify significant differences between 3 sources of error for morphogeometric data: within-observer 1 and 2 (within-obs.1, within-obs.2), and among-observers (among-obs.), compared to and among-genus variability. Asterisk (*) denotes significance.

(within-obs.1 and within-obs.2). While among observer variability is higher than personal error, it is still non-significant (Table 4). It is worth mentioning that measurement error tests using TPS were carried out in a previous study (see supplementary material in⁴⁴), which also indicated a negligible variation compared to inter-genus variation.

In a second analysis, to further assess the robustness of morphometric quantification, we tested variation on landmark data by intentionally misplacing a landmark. For this, LM 15 was slightly moved from its original position by one of the observers. Among-observers variability was tested considering both landmark and semilandmark configuration and only landmarks (excluding semilandmark curves). The former, increased as expected (0.032), although it remains non-significant with respect to inter-generic variation. However, variability considering only landmark configuration was higher (0.041), highlighting the importance of the location of

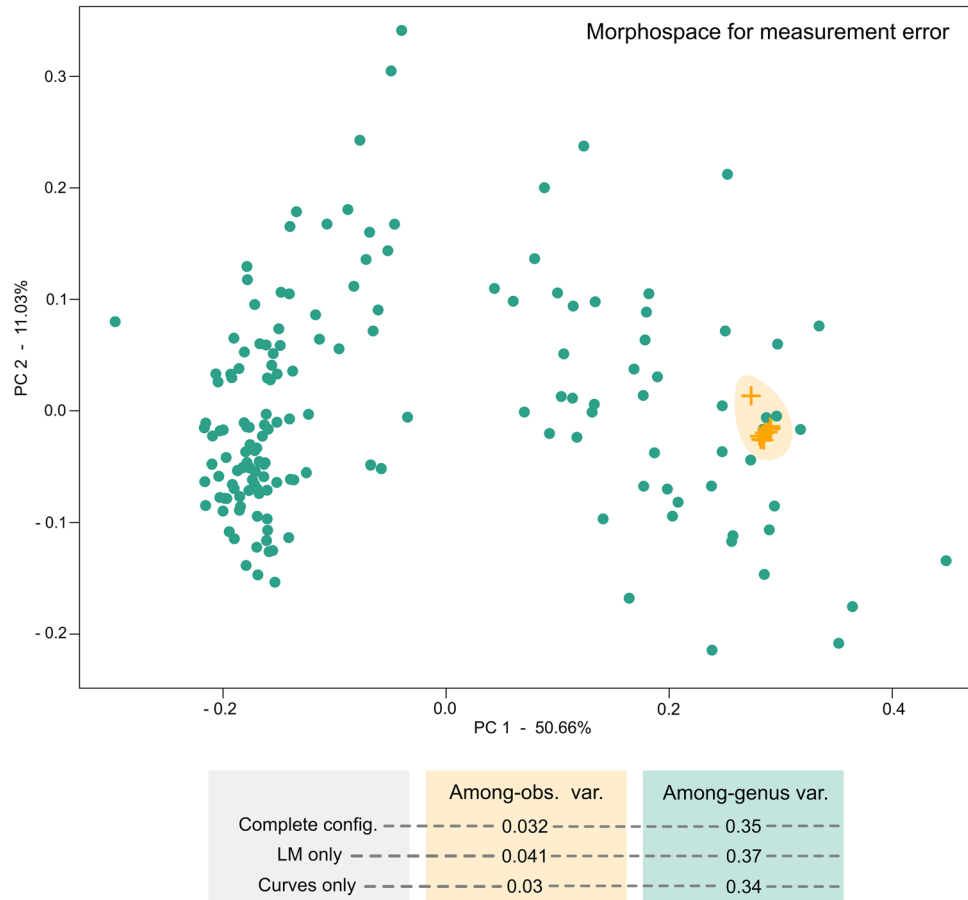


Fig. 8 Morphological variability among specimens considering among-genus and among-observers sources of error. Note the increase in morphological variability among-observers when slightly changing the location of a landmark that makes up for the ending point of a semilandmark curve (orange shade). Abbreviations: config.: configuration, LM: landmarks; obs.: observer, var.: variability.

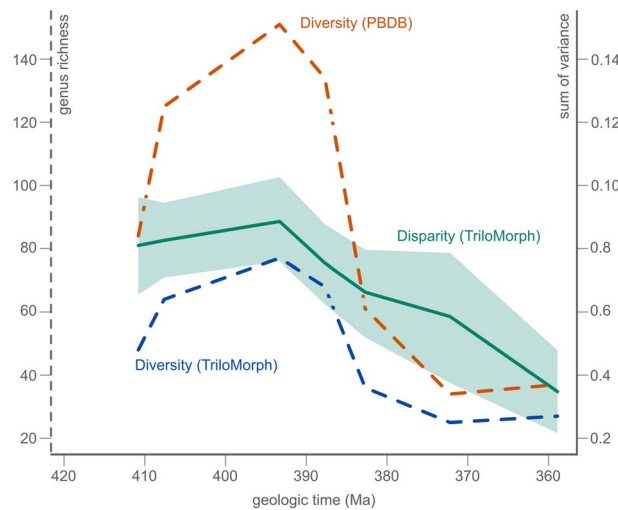


Fig. 9 Devonian disparity and diversity trends based on TriloMorph morphometric data (measured as the SoV) and on trilobite genera present in the PBDB and in TriloMorph respectively.

landmarks that make up for the ending points of semilandmark curves (Fig. 8). Thus special consideration must be taken in the positioning of these landmarks.

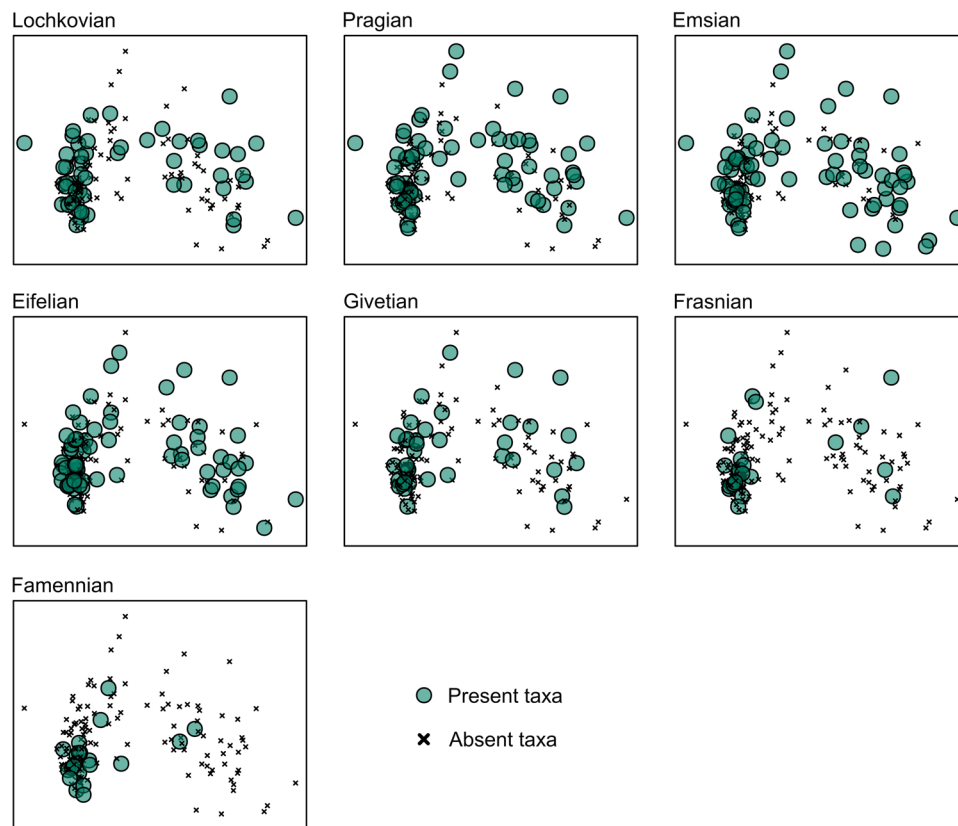


Fig. 10 Morphospace for Lochkovian - Famennian trilobites using data from TriloMorph. Accentuated data points indicate morphotypes present in the respective intervals, morphotypes that are absent (x) are also indicated in order to show the total spectrum.

These results indicate that at the current scale of the dataset, sources of error in the morphogeometric data are much smaller than the natural variability of the data. Therefore our protocol for obtaining data digitised by different contributors is reliable for large scale analyses. Our results are further supported by previous analysis using the same landmarking protocol⁴⁸ where measurement error was lower than within species variability and significantly lower than among genera variability for a single morphologically conservative family (i.e. Phacopidae)⁴⁴.

Finally, part of the database has already been used to investigate trends of morphological disparity of a specific group of Devonian trilobites⁴⁴ and ecological dynamics of late Cambrian–early Ordovician trilobite assemblages⁷⁷, therefore showing the applicability of our database and the usage notes discussed below.

The database is hosted on github⁶² and will be maintained on the long-term by DB, FS and other members of the database.

Usage Notes

A database for morphological information of trilobites is presented herein. The database is open-access with the possibility to download information of interest and/or contribute to the dataset. Researchers who use the database are asked to cite this publication; we strongly encourage users to acknowledge main contributors to the analysed dataset. This novel database is ideal for quantitative analyses regarding morphological diversity, providing an excellent opportunity to explore macroevolutionary and macroecological dynamics.

Nowadays, geometric morphometric analyses are routinely used and there exist several softwares with various capabilities and options to perform such analyses (e.g. MorphoJ⁹⁹, Morphueus¹⁰⁰, PAST¹⁰¹), as well as several packages (e.g. geomorph⁵⁴, shapes¹⁰², Momocs¹⁰³) for R⁶⁰. As an example, here we show the potential of the database for analysing morphological disparity through time, focusing on the Devonian. For this we follow a classical protocol schematized in Fig. 1 (the corresponding R code is available in the file ‘trilomorph-workflow.R’ provided with the TriloMorph database):

1. Load and match landmark data to the user-specified template, number of landmarks, and number of semi-landmarks for each open curve (e.g. with the function provided with the TriloMorph database). The number of semilandmarks to be placed along the curves will ultimately depend on the user’s desired resolution of the shape data. In this contribution we resampled the 4 curves on the cephalon to 12, 20, 20 and 20 semilandmarks respectively because it was sufficient to fit our scope. Here, we use shape files created with StereoMorph (*.txt) or tpsDig (*.tps), but any other format can be used as long as it can be transformed into the standard array (‘landmark values by dimension by specimen’; see⁶⁴). The function shapFix can be used to easily change the desired

number of semilandmarks for each curve as an argument, and also will warn the user and automatically remove specimens with landmark data not fitting the desired template in order to continue with the general analysis.

2. Landmark data are standardised (superimposition step) by applying a generalised Procrustes analysis (GPA; e.g. the function ‘`gpa`’ in the `geomorph` package), which facilitates the comparison of configurations by eliminating variation associated with differences in their location, orientation and size^{52,104–107}.

3. Superimposed data are ordinated into a morphological space by applying a covariance-based principal component analysis (PCA; e.g. the function ‘`plotTangentSpace`’ in the `geomorph` package) in order to quantify and visualise patterns of shape variation. Actual shapes and/or virtual shapes can be plotted over this morphospace to illustrate and highlight major shape variations (Fig. 6).

4. Last, to quantify the morphospace occupation and its changes through time, we calculated the sum of variances (SoV; Fig. 9), which provides a measure of dispersion around the centroid of the group. Noteworthy, several other disparity indices have been developed to capture different aspects of morphospace occupation, and thus consideration of multiple indices is necessary to fully characterise changes in disparity^{108–110}. These additional indices can be computed with the `disPRity` package¹¹¹. In addition, taxonomic richness was standardised according to the Devonian occurrence records from the PBDB.

In our example, the Devonian data from TriloMorph combined with the PBDB shows correspondence between taxonomic and morphological diversity during the Lower and Middle Devonian, where the highest disparity values are related to moments of high taxonomic diversity (Fig. 9). However, towards the Eifelian–Givetian diversity decreases significantly in relation to disparity, with a clear decoupling during the Frasnian. These trends rule out random extinctions as disparity does not remain stable, rather it slowly decreases towards the Upper Devonian. This, in relation to morphospace occupation patterns (Fig. 10), suggest selective extinctions towards the margin, characterised by moderate reductions of the SoV paired with asymmetric reductions of datapoints¹¹².

For large scale analyses, the dataset is meant to be used in conjunction with occurrence data (obtained from the PBDB for example). Indeed, morphological information from TriloMorph and occurrence and higher taxonomic information from the PBDB can be merged according to the desired taxonomic resolution using the genus or species names (Fig. 1: Data recollection). The ‘TriloMorph-workflow’ R script associated with the database illustrates in detail how to merge together occurrence data (such as from the PBDB) to the TriloMorph geometric data and to analyse them to produce disparity curves for example (see Figs. 4, 5, 9, 10).

Code availability

The R script and functions written by the authors used in the analysis are available at the following GitHub repository: <https://github.com/balsedie/trilomorph>. Analyses have been computed with R version 4.1.3¹¹³ with specific functions (available at Github) and the package `geomorph` version 4.0.1^{57,58}.

Received: 14 June 2023; Accepted: 6 November 2023;

Published online: 29 November 2023

References

- Signor, P. W. & Brett, C. E. The mid-Paleozoic precursor to the Mesozoic marine revolution. *Paleobiology* **10**, 229–245 (1984).
- Klug, C. *et al.* The Devonian nekton revolution: Devonian nekton revolution. *Lethaia* **43**, 465–477 (2010).
- Harper, D. A. T., Zhan, R.-B. & Jin, J. The Great Ordovician Biodiversification Event: Reviewing two decades of research on diversity’s big bang illustrated by mainly brachiopod data. *Palaeoworld* **24**, 75–85 (2015).
- Servais, T. *et al.* The onset of the ‘Ordovician Plankton Revolution’ in the late Cambrian. *Palaeogeogr. Palaeoclimatol. Palaeoecol.* **458**, 12–28 (2015).
- Foote, M. Morphologic patterns of diversification: examples from trilobites. *Palaeontology* **34**, 461–485 (1991).
- Adrain, J. M., Westrop, S. R., Chatterton, B. D. E. & Ramsköld, L. Silurian trilobite alpha diversity and the end-Ordovician mass extinction. *Paleobiology* **26**, 625–646 (2000).
- Peters, S. E. Relative abundance of Sepkoski’s evolutionary faunas in Cambrian–Ordovician deep subtidal environments in North America. *Paleobiology* **30**, 543–560 (2004).
- Waisfeld, B. G. & Balseiro, D. Decoupling of local and regional dominance in trilobite assemblages from northwestern Argentina: new insights into Cambro–Ordovician ecological changes. *Lethaia* **49**, 379–392 (2016).
- Saleh, F. *et al.* Contrasting Early Ordovician assembly patterns highlight the complex initial stages of the Ordovician Radiation. *Sci. Rep.* **12**, 3852 (2022).
- Adrain, J. M., Fortey, R. A. & Westrop, S. R. Post-Cambrian Trilobite Diversity and Evolutionary Faunas. *Science* **280**, 1922–1925 (1998).
- Sepkoski, J. J. A Factor Analytic Description of the Phanerozoic Marine Fossil Record. *Paleobiology* **7**, 36–53 (1981).
- Sepkoski, J. J. Biodiversity: Past, Present, and Future. *J. Paleontol.* **71**, 533–539 (1997).
- Alroy, J. Geographical, environmental and intrinsic biotic controls on Phanerozoic marine diversification. *Palaeontology* **53**, 1211–1235 (2010).
- Foote, M., Cooper, R. A., Crampton, J. S. & Sadler, P. M. Diversity-dependent evolutionary rates in early Palaeozoic zooplankton. *Proc. R. Soc. B Biol. Sci.* **285**, 20180122 (2018).
- Fan, J. *et al.* A high-resolution summary of Cambrian to Early Triassic marine invertebrate biodiversity. *Science* **367**, 272–277 (2020).
- Clapham, M. E. Conservation evidence from climate-related stressors in the deep-time marine fossil record. *Philos. Trans. R. Soc. B Biol. Sci.* **374**, 20190223 (2019).
- Finnegan, S. Paleontological baselines for evaluating extinction risk in the modern oceans. *Science* **348**, 567–570.
- The Paleobiology Database. www.paleobiodb.org.
- Geobiodiversity Database. www.geobiodiversity.com.
- Hopkins, M. J. The environmental structure of trilobite morphological disparity. *Paleobiology* **40**, 352–373 (2014).
- Klug, C., De Baets, K., Naglik, C. J. & Waters, J. A new species of *Tiaracrinus* from the latest Emsian of Morocco and its phylogeny. *Acta Palaeontol. Pol.* **59**, 135–145 (2014).
- Holland, S. M. & Sclafani, J. A. Phanerozoic diversity and neutral theory. *Paleobiology* **41**, 369–376 (2015).

23. Balseiro, D. & Powell, M. G. Carbonate collapse and the late Paleozoic ice age marine biodiversity crisis. *Geology* **48**, 118–122 (2019).
24. Moharrek, F. *et al.* Diversification dynamics of cheilostome bryozoans based on a Bayesian analysis of the fossil record. *Palaentology* **65**, e12586 (2022).
25. Albouy, C. *et al.* The marine fish food web is globally connected. *Nat. Ecol. Evol.* **3**, 1153–1161 (2019).
26. Cole, S. R. & Hopkins, M. J. Selectivity and the effect of mass extinctions on disparity and functional ecology. *Sci. Adv.* **7**, eabf4072 (2021).
27. Foote, M. Perimeter-Based Fourier Analysis: A New Morphometric Method Applied to the Trilobite Cranium. *J. Paleontol.* **63**, 880–885 (1989).
28. Foote, M. Morphological and taxonomic diversity in a clade's history: the blastoid record and stochastic simulations. *Contrib. Mus. Paleontol. Univ. Mich.* **28**, 101–140.
29. Foote, M. Contributions of Individual Taxa to Overall Morphological Disparity. *Paleobiology* **19**, 403–419 (1993).
30. Foote, M. The Evolution of Morphological Diversity. *Annu. Rev. Ecol. Syst.* **28**, 129–152 (1997).
31. Foote, M. Discordance and concordance between morphological and taxonomic diversity. *Paleobiology* **19**, 185–204 (1993).
32. Roy, K. & Foote, M. Morphological approaches to measuring biodiversity. *Trends Ecol. Evol.* **12**, 277–281 (1997).
33. Neige, P. Spatial patterns of disparity and diversity of the recent cuttlefishes (Cephalopoda) across the Old World. *J. Biogeogr.* **30**, 1125–1137 (2003).
34. Benton, M. J. Exploring macroevolution using modern and fossil data. *Proc. R. Soc. B Biol. Sci.* **282**, 20150569 (2015).
35. Maestri, R., Monteiro, L. R., Fornel, R., de Freitas, T. R. O. & Patterson, B. D. Geometric morphometrics meets metacommunity ecology: environment and lineage distribution affects spatial variation in shape. *Ecography* **41**, 90–100 (2018).
36. Gonzalez, P. N. *et al.* Description and Analysis of Spatial Patterns in Geometric Morphometric Data. *Evol. Biol.* **46**, 260–270 (2019).
37. Jablonski, D. Developmental bias, macroevolution, and the fossil record. *Evol. Dev.* **22**, 103–125 (2019).
38. Madin, J. S. *et al.* The Coral Trait Database, a curated database of trait information for coral species from the global oceans. *Sci. Data* **3**, 160017 (2016).
39. Davies, C. H. *et al.* A database of marine phytoplankton abundance, biomass and species composition in Australian waters. *Sci. Data* **3**, 160043 (2016).
40. Raja, N. B., Dimitrijević, D., Krause, M. C. & Kiessling, W. Ancient Reef Traits, a database of trait information for reef-building organisms over the Phanerozoic. *Sci. Data* **9**, 425 (2022).
41. Hopkins, M. J., Wagner, P. J. & Jordan, K. J. Permian trilobites and the applicability of the “living fossil” concept to extinct clades. *Front. Ecol. Evol.* **11**, (2023).
42. Suárez, M. G. & Esteve, J. Morphological diversity and disparity in trilobite cephalons and the evolution of trilobite enrolment throughout the Palaeozoic. *Lethaia* **54**, 752–762 (2021).
43. Holmes, J. D. Contrasting patterns of disparity suggest differing constraints on the evolution of trilobite cephalic structures during the Cambrian ‘explosion’. *Palaentology* **66**, e12647 (2023).
44. Bault, V. *et al.* Rise and fall of the phacopids: the morphological history of a successful trilobite family. *Palaentology* **66**, e12673 (2023).
45. Drage, H. B. Trilobite moulting behaviour variability had little association with morphometry. *bioRxiv* 2022.12.12.520015, <https://doi.org/10.1101/2022.12.12.520015> (2022).
46. Adrain, J. M. *et al.* Trilobites. in *The Great Ordovician Biodiversification Event* (eds. Webby, B. D., Paris, F., Droser, M. L. & Percival, I. G.) 231–254 (Columbia University Press, 2004).
47. Zhang, S., Fan, J., Morgan, C. A., Henderson, C. M. & Shen, S. Quantifying the middle–late Cambrian trilobite diversity pattern in South China. *Palaogeogr. Palaeoclimatol. Palaeoecol.* **570**, 110361 (2021).
48. Bault, V., Crónier, C. & Monnet, C. Morphological disparity trends in Devonian trilobites from North Africa. *Palaentology* **65**, e12623 (2022).
49. Lerosey-Aubril, R. & Feist, R. Quantitative Approach to Diversity and Decline in Late Palaeozoic Trilobites. in *Earth and Life* (ed. Talent, J. A.) 535–555, https://doi.org/10.1007/978-90-481-3428-1_16 (Springer Netherlands, 2012).
50. Paterson, J. R. The trouble with trilobites: classification, phylogeny and the cryptogenesis problem. *Geol. Mag.* **157**, 35–46 (2020).
51. Bault, V., Balseiro, D., Monnet, C. & Crónier, C. Post-Ordovician trilobite diversity and evolutionary faunas. *Earth-Sci. Rev.* **230**, 104035 (2022).
52. Zelditch, M. L., Swiderski, D. L. & Sheets, H. D. *Geometric Morphometrics for Biologists: a primer*. <https://doi.org/10.1016/B978-0-12-386903-6.00001-0> (Elsevier, 2012).
53. Hopkins, M. & Pearson, J. Non-linear ontogenetic shape change in *Cryptolithus tessellatus* (Trilobita) using three-dimensional geometric morphometrics. *Palaentol. Electron.* **19**, 3, 1–54 (2016).
54. Adams, D. C. & Otárola-Castillo, E. geomorph: an R package for the collection and analysis of geometric morphometric shape data. *Methods Ecol. Evol.* **4**, 393–399 (2013).
55. Schneider, C. A., Rasband, W. S. & Eliceiri, K. W. NIH Image to ImageJ: 25 years of image analysis. *Nat. Methods* **9**, 671–675 (2012).
56. Rohlf, F. J. The tps series of software. *Hystrix Ital. J. Mammal.* **26**, 9–12 (2015).
57. Baken, E. K., Collyer, M. L., Kaliontzopoulou, A. & Adams, D. C. geomorph v4.0 and gmShiny: Enhanced analytics and a new graphical interface for a comprehensive morphometric experience. *Methods Ecol. Evol.* **12**, 2355–2363 (2021).
58. Adams, D. C., Rohlf, F. J. & Slice, D. E. Geometric morphometrics: Ten years of progress following the ‘revolution’. *Ital. J. Zool.* **71**, 5–16 (2004).
59. Olsen, A. M. & Westneat, M. W. StereoMorph: an R package for the collection of 3D landmarks and curves using a stereo camera set-up. *Methods Ecol. Evol.* **6**, 351–356 (2015).
60. R Core Team. R: The R Project for Statistical Computing. R Foundation for Statistical Computing, Vienna, Austria. (2018).
61. Serra, F. *et al.* A dynamic and collaborative database for morphogeometric information of trilobites. *Repositorio Digital UNC* <https://rdu.unc.edu.ar/handle/11086/547753> (2023).
62. Serra, F. *et al.* *TriloMorph*. balsedie/trilomorph: stable_release (v1.0). *Zenodo* <https://doi.org/10.5281/zenodo.8033445> (2023).
63. The Official YAML Web Site. www.yaml.org.
64. Claude, J. *Morphometrics with R*. (Springer, 2008).
65. Waisfeld, B. G. & Vaccari, N. E. Trilobites. in *Ordovician Fossils of Argentina* (ed. Benedetto, J. L.) 295–410 (Secretaría de Ciencia y Tecnología - Universidad Nacional de Córdoba, 2003).
66. Waisfeld, B. G., Vaccari, N. E., Chatterton, B. D. E. & Edgcombe, G. D. Systematics of Shumardiidae (Trilobita), with new species from the Ordovician of Argentina. *J. Paleontol.* **75**, 827–859 (2001).
67. Vaccari, N. E. & Waisfeld, B. G. *Kainella* Walcott, 1925 (Trilobita, Ordovícico Temprano) en el noroeste de Argentina y sur de Bolivia. *Paleontología sistemática. Ameghiniana* **47**, 273–292 (2010).
68. Meroi Arcerito, F. R., Waisfeld, B. & Balseiro, D. Diversification of *Asaphellus* Callaway, 1877 (Asaphidae: Trilobita) during the Tremadocian in South West Gondwana (Cordillera Oriental, Argentina). *Geodiversitas* **37**, 131–150 (2015).
69. Arcerito, F. R. M., Waisfeld, B. G., Vaccari, N. E. & Muñoz, D. F. High Resolution Trilobite Biostratigraphy for the Early Late Tremadocian (Tr2) Interval (Early Ordovician) Santa Rosita Formation, Argentine Cordillera Oriental. *Ameghiniana* **55**, 531 (2018).

70. Rustán, J. J., Balseiro, D., Waisfeld, B., Foglia, R. D. & Vaccari, N. E. Infaunal molting in Trilobita and escalatory responses against predation. *Geology* **39**, 495–498 (2011).
71. Rustán, J. J. & Vaccari, N. E. The Aulacopleurid Trilobite *Maurotarion* Alberti, 1969, in the Silurian-Devonian of Argentina: Systematic, Phylogenetic and Paleobiogeographic Significance. *J. Paleontol.* **84**, 1082–1098 (2010).
72. Rustán, J. J. & Balseiro, D. The phacopid trilobite *Echidnops taphominus* n. sp. from the Lower Devonian of Argentina: insights into infaunal molting, eye architecture and geographic distribution. *J. Paleontol.* **90**, 1100–1111 (2016).
73. Rustán, J. J. & Vaccari, N. E. A revision of the Devonian Malvinokaffric dalmanitid trilobite *Dalmanitoides* Delo, 1935, on the basis of new data from Argentina. *Palaeontol. Electron.* **15**, 21 (2012).
74. Randolfe, E. A., Rustán, J. J. & Bignon, A. A taxonomic revision of the Early Devonian dalmanitid trilobite *Kasachstania* Maksimova, 1972 from central Kazakhstan. *J. Paleontol.* **94**, 681–695 (2020).
75. Randolfe, E. A., Rustán, J. J. & Bignon, A. New dalmanitid trilobite taxa from the Lower Devonian of Argentina: comments on spinosity in endemic taxa from southern high paleolatitudes. *Comptes Rendus Palevol* **21**, 17–38 (2022).
76. Rustán, J. J., Waisfeld, B. G. & Vaccari, N. E. The homalonotid trilobite *Burmeisteria* Salter, 1865 in the Lower Devonian of Argentina: new data in the context of southwestern Gondwana. *J. Paleontol.* **94**, 498–512 (2020).
77. Serra, F., Balseiro, D. & Waisfeld, B. G. Morphospace trends underlying a global turnover: Ecological dynamics of trilobite assemblages at the onset of the Ordovician Radiation. *Palaeogeogr. Palaeoclimatol. Palaeoecol.* **615**, 111448 (2023).
78. Bignon, A., Waisfeld, B. G., Vaccari, N. E. & Chatterton, B. D. E. Reassessment of the Order Trinucleida (Trilobita). *J. Syst. Palaeontol.* **18**, 1061–1077 (2020).
79. Bignon, A., Corbacho, J. & López-Soriano, F. J. A revision of the first Asteropyginae (Trilobita; Devonian). *Geobios* **47**, 281–289 (2014).
80. Bignon, A. & Crônier, C. Evolutionary modifications of ontogeny of three *Dechenella* species (Proetidae), from the Middle Devonian of the Ardenne Massif (France). *J. Paleontol.* **86**, 558–566 (2012).
81. Bignon, A. & Crônier, C. The systematics and phylogeny of the Devonian subfamily Asteropyginae (Trilobita: Phacopida). *J. Syst. Palaeontol.* **12**, 637–668 (2014).
82. Crônier, C. Morphological disparity and developmental patterning: contribution of phacopid trilobites. *Palaeontology* **56**, 1263–1271 (2013).
83. Crônier, C., Feist, R. & Auffray, J.-C. Variation in the eye of *Acuticryphops* (Phacopina, Trilobita) and its evolutionary significance: a biometric and morphometric approach. *Paleobiology* **30**, 471–481 (2004).
84. Crônier, C., Bignon, A. & François, A. Morphological and ontogenetic criteria for defining a trilobite species: The example of Siluro-Devonian Phacopidae. *Comptes Rendus Palevol* **10**, 143–153 (2011).
85. Crônier, C., Renaud, S., Feist, R. & Auffray, J.-C. Ontogeny of *Trimeroccephalus lelievrei* (Trilobita, Phacopida), a representative of the Late Devonian phacopine paedomorphocline: a morphometric approach. *Paleobiology* **24**, 359–370 (1998).
86. Crônier, C., Ariuntogos, M., Königshof, P., Waters, J. A. & Carmichael, S. K. Late Devonian (Famennian) phacopid trilobites from western Mongolia. *Palaeobiodiversity Palaeoenvironments* **101**, 707–723 (2021).
87. Kim, K., Sheets, H. D., Haney, R. A. & Mitchell, C. E. Morphometric analysis of ontogeny and allometry of the Middle Ordovician trilobite *Triarthrus becki*. *Paleobiology* **28**, 364–377 (2002).
88. Sheets, H. D., Kim, K. & Mitchell, C. E. A combined landmark and outline-based approach to ontogenetic shape change in the Ordovician trilobite *Triarthrus becki*. in *Morphometrics: Applications in Biology and Paleontology* (ed. Elewa, A. M. T.) 67–82, https://doi.org/10.1007/978-3-662-08865-4_6 (Springer, 2004).
89. Fusco, G., Hughes, N. C., Webster, M. & Minelli, A. Exploring developmental modes in a fossil arthropod: growth and trunk segmentation of the trilobite *Aulacopleura konincki*. *Am. Nat.* **163**, 167–183 (2004).
90. Crônier, C. & Fortey, R. A. Morphology and ontogeny of an early Devonian phacopid trilobite with reduced sight from Southern Thailand. *J. Paleontol.* **80**, 529–536 (2006).
91. Webster, M. & Sheets, H. D. A Practical Introduction to Landmark-Based Geometric Morphometrics. *Paleontol. Soc. Pap.* **16**, 163–188 (2010).
92. MacLeod, N. Landmarks, Localization, and the Use of Morphometrics in Phylogenetic Analysis. in *Fossils, Phylogeny, and Form: An Analytical Approach* (eds. Adrain, J. M., Edgecombe, G. D. & Lieberman, B. S.) 197–233, https://doi.org/10.1007/978-1-4615-0571-6_6 (Springer US, 2001).
93. Webster, M. & Zelditch, M. L. Modularity of a Cambrian ptychoparioid trilobite cranium: Modularity of trilobite cranium. *Evol. Dev.* **13**, 96–109 (2011).
94. Gendry, D., Courville, P., Saucède, T., Laffont, R. & Paris, F. Contribution of Morphometrics to the Systematics of the Ordovician Genus *Neseuretus* (Calymenidae, Trilobita) from the Armorican Massif, France. *J. Paleontol.* **87**, 456–471 (2013).
95. Esteve, J., Gutiérrez-Marco, J. C., Rubio, P. & Rábano, I. Evolution of trilobite enrolment during the Great Ordovician Biodiversification Event: insights from kinematic modelling. *Lethaia* **51**, 207–217 (2018).
96. Whittington, H. B. Morphology of the exoskeleton. in *Treatise on invertebrate paleontology. Part O, Arthropoda 1, Trilobita revised* (ed. Kaesler, R. L.) vol. 1 1–85 (The Geological Society of America & The University of Kansas, Boulder, Colorado & Lawrence, 1997).
97. Fortey, R. A. & Owens, R. M. Evolutionary history. in *Treatise on Invertebrate Paleontology. Part O, Arthropoda 1, Trilobita* (ed. Kaesler, R. L.) 250–287 (The Geological Society of America & University of Kansas, Boulder, Colorado & Lawrence, 1997).
98. Anderson, M. J. Distance-based tests for homogeneity of multivariate dispersions. *Biometrics* **62**, 245–253 (2006).
99. Klingenberg, C. P. MorphoJ: an integrated software package for geometric morphometrics. *Mol. Ecol. Resour.* **11**, 353–357 (2011).
100. Slice, D. E. *Morpheus et al.*, Java Edition (2013).
101. Hammer, O., Harper, D. A. T. & Ryan, P. D. PAST: Paleontological Statistics Software Package for Education and Data Analysis. *Palaeontol. Electron.* **4**, (2001).
102. Dryden, I. L. Shapes package. R Foundation for Statistical Computing, Vienna, Austria. Contributed package. (2021).
103. Bonhomme, V., Picq, S., Gaucherel, C. & Claude, J. Momocs: Outline Analysis Using R. *J. Stat. Softw.* **56**, 1–24 (2014).
104. Gower, J. C. Generalized procrustes analysis. *Psychometrika* **40**, 33–51 (1975).
105. Rohlf, F. J. & Slice, D. Extensions of the Procrustes Method for the Optimal Superimposition of Landmarks. *Syst. Zool.* **39**, 40 (1990).
106. Bookstein, F. L. *Morphometric Tools for Landmark Data: Geometry and Biology*. <https://doi.org/10.1017/CBO9780511573064> (Cambridge University Press, 1992).
107. O’Higgins, P. The study of morphological variation in the hominid fossil record: biology, landmarks and geometry. *J. Anat.* **197**, 103–120 (2000).
108. Wills, M. A., Briggs, D. E. G. & Fortey, R. A. Disparity as an Evolutionary Index: A Comparison of Cambrian and Recent Arthropods. *Paleobiology* **20**, 93–130 (1994).
109. Ciampaglio, C. N., Kemp, M. & McShea, D. W. Detecting Changes in Morphospace Occupation Patterns in the Fossil Record: Characterization and Analysis of Measures of Disparity. *Paleobiology* **27**, 695–715 (2001).
110. Guillerme, T. et al. Disparities in the analysis of morphological disparity. *Biol. Lett.* **16**, 20200199 (2020).
111. Guillerme, T. dispRity: A modular R package for measuring disparity. *Methods Ecol. Evol.* **9**, 1755–1763 (2018).
112. Korn, D., Hopkins, M. J. & Walton, S. A. Extinction space—a method for the quantification and classification of changes in morphospace across extinction boundaries: extinction space. *Evolution* **67**, 2795–2810 (2013).

113. R Core Team. R: A language and environment for statistical computing. R Foundation for Statistical Computing, Vienna, Austria. (2022).
114. Gon, S. M. III A pictorial guide to the Orders of trilobites. <http://www.trilobites.info/>. (2009).
115. Scotese, C. R. PALEOMAP website. <http://www.scotese.com> (2002).
116. Müller, R. D. *et al.* GPlates: Building a Virtual Earth Through Deep Time. *Geochem. Geophys. Geosystems* **19**, 2243–2261 (2018).

Acknowledgements

This publication is part of an ECOS Sud-MinCyT project co-financed by the Ministère de l'Europe et des Affaires Étrangères (MEAE) and the Ministère de l'Enseignement Supérieur et de la Recherche et de l'Innovation (MESRI) on behalf of France and the Ministerio de Ciencia, Tecnología e Innovación on behalf of Argentina (n°A17A01). We wish to express our appreciation to the editorial team, Dr Harriet B. Drage and an anonymous reviewer whose insightful comments greatly improved this contribution. A.B., B.G.W., D.B., D.F.M., E.N.V., E.R., F.S., and J.J.R. acknowledge supporting facilities of the Consejo Nacional de Investigaciones Científicas y Técnicas and Universidad Nacional de Córdoba. E.R would like to thank the Národní Muzeum for allowing, in collaboration with Synthesys+, access to specimens included in TriloMorph. The authors would like to thank Axelle Zacaï (PALEVOPRIM, Poitiers Univ., France) and Nicolás Wolovick (FaMAF, UNC) for useful discussions regarding the database structure, and to Sam Gon III for allowing the use of his figures. This is Paleobiology Database official publication number #473. This contribution has been possible thanks to the financial support of the international collaboration ECOS-Sud project n°A17A01 (France-Argentina). Financial support for this study was further provided by the ANPCyT-FONCyT PICT 2019-01818 to FS and PICT-2021-I-A-00968 to DB; CONICET PIP 202111220200103192 to BGW and DB; and the Synthesys + Project (Transnational Access) and the Paleontological Society (Sepkoski Award) to ER.

Author contributions

C.C. and B.G.W. led the project and were responsible for funding support. C.C., B.G.W., A.B., J.J.R., F.S., N.E.V. and D.B. designed the landmarking protocol. D.B., A.B., C.C., F.S. and D.F.M. designed the dataset. F.S., D.B., E.R., D.F.M., V.B., J.J.R., N.E.V., A.B., B.G.W. and C.C. organised and carried out the data collection. C.M. wrote the R functions used to perform the morphological analyses. C.M. analysed the data with input from F.S. and D.B. D.B. designed and built the Github repository with input from F.S., F.S., D.B. and C.M. wrote the manuscript with input from all the authors.

Competing interests

The authors declare no competing interests.

Additional information

Supplementary information The online version contains supplementary material available at <https://doi.org/10.1038/s41597-023-02724-9>.

Correspondence and requests for materials should be addressed to C.C. or B.G.W.

Reprints and permissions information is available at www.nature.com/reprints.

Publisher's note Springer Nature remains neutral with regard to jurisdictional claims in published maps and institutional affiliations.



Open Access This article is licensed under a Creative Commons Attribution 4.0 International License, which permits use, sharing, adaptation, distribution and reproduction in any medium or format, as long as you give appropriate credit to the original author(s) and the source, provide a link to the Creative Commons licence, and indicate if changes were made. The images or other third party material in this article are included in the article's Creative Commons licence, unless indicated otherwise in a credit line to the material. If material is not included in the article's Creative Commons licence and your intended use is not permitted by statutory regulation or exceeds the permitted use, you will need to obtain permission directly from the copyright holder. To view a copy of this licence, visit <http://creativecommons.org/licenses/by/4.0/>.

© The Author(s) 2023